American Journal of Materials Science and Application
2015; 3(2): 18-25
Published online February 20, 2015 (http://www.openscienceonline.com/journal/ajmsa)

Corrosion Behaviour of Titanium Nitride Coating on Titanium and Zircaloy-4

P. M. Perillo

Micro and Nanotechnology, Atomic Energy National Commision, Buenos Aires, Argentina

Email address

perillo@cnea.gov.ar

To cite this article

P. M. Perillo. Corrosion Behaviour of Titanium Nitride Coating on Titanium and Zircaloy-4. *American Journal of Materials Science and Application*. Vol. 3, No. 2, 2015, pp. 18-25.

Abstract

The present study deals with growth of TiN coatings deposited by plasma enhanced physical vapor deposition (PEPVD) on commercial titanium substrate and zircaloy-4. The composition, microstructure and residual stresses of the coatings were determined by scanning electron microscopy (SEM), photoelectron spectroscopy generated by X-rays (XPS/ ESCA) and X-ray diffraction. The anodic behaviour of TiN layers were investigated by means of potentiodynamic anodic polarization curves and galvanostatic experiments, in 0.1M NaCl solution at room temperature. The results were compared with those obtained for the non-coated materials in the same experimental conditions. Results showed that in the corrosive media tested the anodic behaviour of the coated materials was somewhat different from the anodic behaviour of the uncoated material. However, the corrosion performance of both titanium and Zyr-4 is not markedly modified by the TiN coating. In another series of experiments the electronic properties of the coating were investigated by measuring the anodic and cathodic polarization curves in a solution containing a redox system (Na_2SO_4 0,1M + $K_4[Fe(CN)_6]$ 0,05M+ $K_3[Fe(CN)_6]$ 0,05M). The TiN film possess an electronic conductivity higher than the electronic conductivity of the oxide film present on the Ti and Zyr-4 surface, therefore may be used in applications where a good electrical conductivity is required

Keywords

Corrosion, TiN, Ti, Zry-4, PEPVD, Electronic Conductivity, Coating

1. Introduction

The ability to protect against corrosion of the coatings produced by PVD is widely discussed in the literature [1-5].

The TiN coating prepared by PEPVD is one of the hard coatings most used at present. Its excellent combination of properties such as wear resistance, low chemical reactivity, resistance to temperature, gold metallic, low coefficient of friction, make it attractive for a wide variety of applications. Thin films of TiN are also used in microelectronics, where they serve as a conductive barrier between the active device and the metal contacts used to operate the circuit. The film blocks the diffusion of metal of the conductor into the silicon, but it is conductive enough (30–70 μΩ·cm) to allow a good electrical connection.

The materials used as substrate materials are very varied and may include among other tool steels, stainless steels, nickel alloys, aluminium alloys, etc.

Numerous works were found in the literature devoted to study the changes in the corrosion behaviour of steel and Ti alloys when coated with TiN [6]-[23]. However, despite the unusually low electrical resistivity of TiN coatings (25-40 μΩ.cm), there is a research aiming to explore the possibility of using TiN coatings in applications where the existence of a coating with good electrical conductivity applied on a substrate with insulating characteristics is required. This paper aims to assess the changes introduced by the coating of TiN on the behaviour of substrates such as Ti and Zyr-4 [24,25], which have a high corrosion resistance due to the presence on its surface of a protective oxide film with insulator electronic properties.

2. Experimental Procedure

2.1. Coatings Preparation

The coatings were deposited by PEPVD in a R3-J RMP3 Nissin Electric equipment. After cleaning, the samples were inserted into the carrier substrate, the vacuum chamber was evacuated to approximately 6.6 x 10^{-3} Pa. The temperature was controlled by a chromel alumel thermocouple. The coatings were deposited with a cathode arc current of 80 A with a negative substrate bias of 300 V and a substrate current of 1 A. Cathode was used as pure titanium (99.8%). A mixture of argon and nitrogen in ratio 1:30 was used and the total pressure in the chamber was 3.99 Pa. The TiN coating include a thin pre-deposited (< 200 nm) metallic Ti interlayer. After 15 minutes the temperature was raised to 300 °C and then remained constant. The thickness of the coatings was controlled by deposition time.

Sheets of commercially pure grade titanium (99.8%) and Zyr-4 have dimensions of 15 mm x 10 mm x 2 mm thick. Prior to experiments, the titanium sheets were firstly smoothed and cleaned using sandpaper, then the foils were ultrasonically cleaned in isopropyl alcohol and acetone solution, afterwards rinsed with deionized water and finally dried in a nitrogen stream.

Double-layered and four-layered TiN coatings were obtained by repeating the same process for two or four multiple runs, therefore they consisted of two or four consecutive single layer treatments [26].

2.2. Characterization of TiN Coating

The composition, morphology, microstructure, adhesion and hardness of the coatings were determined. The thickness of the coating was measured using the Calotest method [27].

Scanning electron microscope (Fei model Quanta 200) was employed for the morphological charactherization of the TiN coatings.

X-ray diffraction (XRD) patterns were recorded at room temperature with Cu Kα radiation of 0.15418 nm in a diffractometer (Philips X'Pert) using conventional Bragg-Brentano (BB) diffraction geometry. The data were collected for scattering angles (2θ) ranging from 20° to 120° with a step 2θ of 0.02° for 1 s by step.

The coating chemical elements and their bonding condition were characterized using X-ray photoelectron spectroscopy (XPS) [28]. (Vacuum Generator Mod. ESCA 3 MARK II) The X-ray in XPS was generated at 10 kV and 20 mA, using Mg Kα radiation (hv=1253.6 eV). The air pressure in the vacuum chamber was 7×10^{-9} Torr. The depth profile analysis of the near surface regions were carried out by sputtering with Ar^+ ions using a current intensity of 6 μA and an acceleration voltage of 5 kV (ion current, 8 μA) at an argon pressure of 8×10^{-5}mTorr. All the experiments were conducted at room temperature.

The microhardness measurements were performed with an Akashi microhardness tester (MVK-H2). In order to prevent from substrate effect a load of 25 gf was applied to the sample and 10 measurements were made and the average was taken as the representative value.

A CSEM-REVETEST scratch tester was used to determine the adhesion characteristics. The scratch tests were performed under the standard conditions (diamond stylus R = 0.2 mm; scratching speed 10mm/min; loading rate 100 N/min). In the scratch experiments, we measured the scratch channel widthand from this value calculated the scratch depth 6 from trigonometry as a function of the applied load considering a spherical indenter with a measured radius of 200 pm.

Corrosion behaviour of the coatings was investigated by potentiodynamic polarization tests in 0.1 M NaCl at room temperature. The corrosion resistance of samples was tested by using a Gamry PC4/750 potentiostat/galvanostat analyzer. The electronic properties of the coating were investigated by measuring the anodic and cathodic polarization curves in a solution containing a redox system (Na_2SO_4 0,1M + $K_4[Fe(CN)_6]$ 0,05M+ $K_3[Fe(CN)_6]$ 0,05M).

3. Results and Discussion

3.1. Crystalline Phases

Figure 1 shows the phases present in the coating and the substrate. Diffraction peaks are located in the crystallographic planes (111), (200), (220) and (311) at angles of 34.2°, 39.8°, 59.1° and 86.1° respectively, characteristic of the fcc structure of TiN [29].

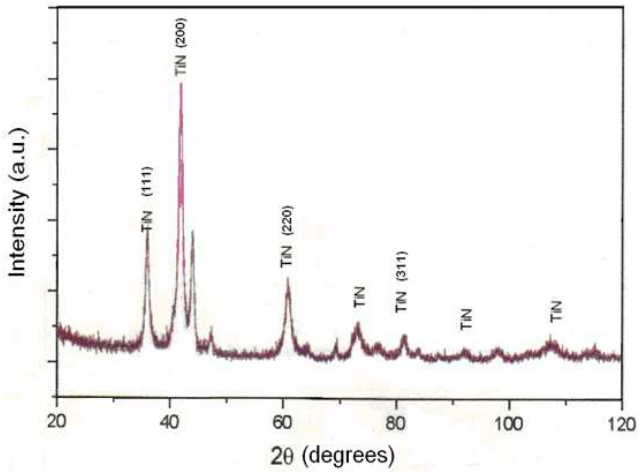

Figure 1. *XRD patterns of TiN coating on Ti.*

3.2. Chemical Characterization

The XPS investigations of the surface of the film show the presence of the elements Ti, N, O and contaminations of C (Fig 2). The C was virtually eliminated with a cleaning sweep during 8 minutes with Ar^+ ions. The atomic percentages of the coating components were determined: N 41,23% O 10,68% and Ti 48,09%. Oxygen presents a significant peak. It is estimated that 10% oxygen incorporated into the coating.

The peaks of titanium Ti2p, nitrogen N1s, oxygen O1s and carbon C1s were investigated in detail and peak position were estimated. The nitrogen N1s binding energy (396,5 eV)

indicates that nitrogen is combinated to form nitrides.

Figure 4 corresponds to oxygen 1s which is combinated as oxides. This signal does not disappear into the coating. The O1s binding is 531,4 eV.

Figure 5 shows the Ti2p XPS spectrum. Ti2p XPS envelope was de-convoluted to 2 doublet peaks which were 454,6 eV and 460 eV. According to the literature data, binding energies of Ti2p XPS peak is characterized by approximately 455 eV for TiN. On the other hand, higher binding energies are associated with increasing oxygen contents in oxy-nitrides and oxides. As oxygen content increases in the oxide phase, stoichiometry and the binding energy approach to the values of TiO_2 [30]. Ti2p consisting of more than one compound: nitrides and oxides.

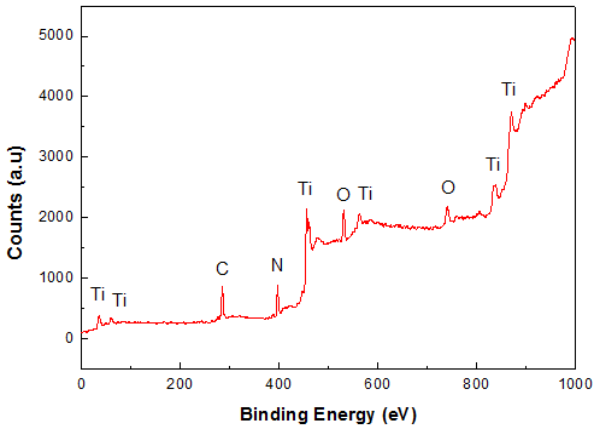

Figure 2. *Wide spectrum of TiN*

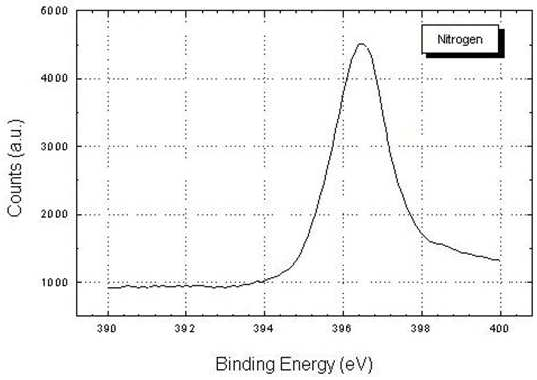

Figure 3. *Narrow spectrum of N corresponding to N 1s*

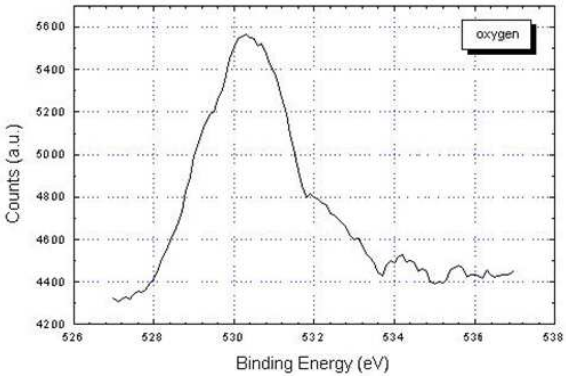

Figure 4. *Narrow spectrum corresponding to O1s*

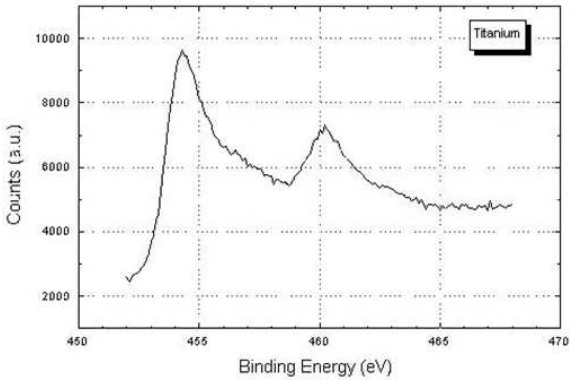

Figure 5. *Deconvoluted Ti2p XPS line of TiN coating*

The fractured section of the coating are shown in Fig 6 a. It can be observed that the TiN exhibits typical columnar microstructure in which grain boundaries grow perpendicular to the substrate surface. Fig 6 b shows the surface morphology of the coating. Significant macroparticles, droplets and growth defects, which were probably formed during sputtering process, can be observed on the surface of the coating in addition to various pinholes and craters. SEM images can prove that selective corrosion occurs at growth defect sites.

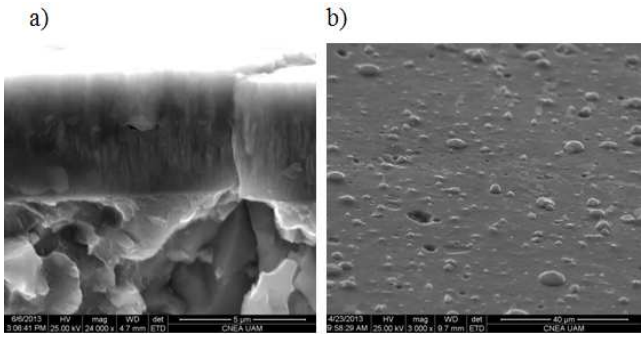

Figure 6. *SEM micrographs of TiN a) cross sectional, b) top view.*

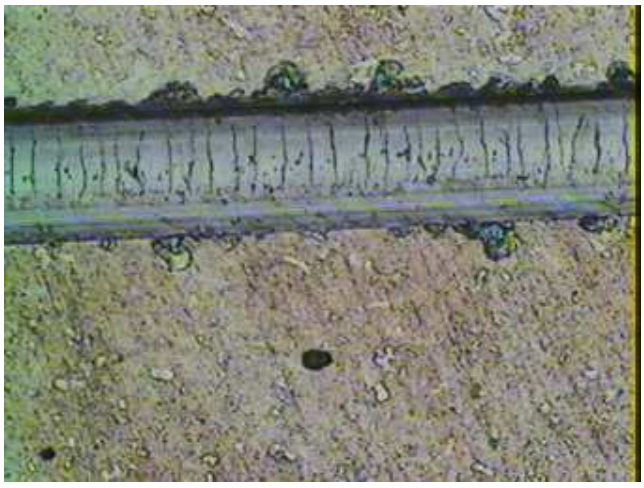

Figure 7. *Optical microscope photographs of failure modes around the scratch channel for TiN coatings on Ti.*

The calculated deposition rate for the coatings was 10 µm/h. The thickness of the coating was 4 µm approximately. The hardness of TiN was 2500-2600 Hv.

Fig. 7 shows the optical microscope photographs of the scratch channel of coatings on Ti prepared by PECVD. Both failure modes are present. The coating failure takes place in the form of large chip fractures (cohesion fractures) at the edge of the scratch channel and flak ing (adhesive failures) between film and substrate occurs. Adhesion of the coatings was found to be 30-35 N.

3.3. Electrochemical Tests

Potentiodynamic anodic polarization curves were obtained by increasing the potential at a scan rate of 0.167 $mV.s^{-1}$ from a potential value 0,05V lower than the corrosion potential. In order to prevent crevice corrosion, the samples were masked with lacquer acetate, leaving a free area of 1 cm^2 in contact with the solution. The solution tested was a 0.1M NaCl solution. Before starting the measurements, the samples were allowed to reach a stationary potential by a 1 h exposure to the solution. Measurements were performed in a conventional three electrode Pyrex glass cell with a platinum count electrode. Potentials were measured through a Lugging capillary, with a calomel saturated reference electrode (SCE). The solutions were de-aerated for 1 h with high purity nitrogen prior to each experiment. The SCE is much lower in deaerated electrolytes. The presence of oxygen thus increases the cathodic current and its corrosion potential. De aeration was continued during the experiments. The solutions were prepared with analytical grade reagents and distilled water. All potentials in the present paper are reported in the standard hydrogen electrode (SHE) scale.

Galvanostic experiments were performed by applying a constant current density of 0.8 $A.cm^{-2}$ and measuring the variation of the potential as a function of time for periods of 3 hs and 24 hs. In another series of experiments the electronic properties of the film coating were investigated by measuring the anodic and cathodic polarization curves of the coated samples in a solution containing a redox couple (0,1M Na_2SO_4 + 0,05M $K_4[Fe(CN)_6]$ + 0,05M $K_3[Fe(CN)_6]$).

3.4. Potentyodinamic Polarization Curves

Commercial Ti y Ti coated with TiN

The anodic potentyodinamic polarization curves obtained for titanium coated with single layer TiN coating and commercial titanium in deaerated 0.1 M NaCl solution are shown in Figure 8.

These curves are similar to those reported by Rossi et al for glow nitrided Ti_6Al_4V alloy in a NaCl solution [12]. Few differences were observed between the behaviour of coated and uncoated samples. The coated samples exhibited an increment of the corrosion potential compared with the non-coated material. On the other hand, the uncoated Ti exhibited the typical passive behaviour originated from the presence of a TiO_2 passivating film on the metal surface. The current density shows a sudden increase when the potential was increased above the corrosion potential, attaining a value of the order of 10^{-6} $A.cm^{-2}$. Further increasing the potential, the current density remained almost constant up to a potential value close to 2,5V. At potential values higher than 2.5 V, the current density augmented gradually as the potential was increased. The increase in current density observed above 2.5 V may be caused by the oxidation of the aqueous media with a consequent oxygen evolution. On the other hand, the coated material showed at low overpotentials, very low anodic current density values, ranging from 10^{-8} to 10^{-7} $A.cm^{-2}$, and more than one order of magnitude lower than the passive current measured for the untreated Ti. However, these values did not remain constant. They grew according to the anodic polarization potential. This current increase was not observed in the polarization curve of the untreated metal and could be related with the oxidation of TiN to TiO_2, according to the reaction (1) [31-32]:

$$TiN + 2\ H_2O \rightarrow TiO_2 + ½\ N_2 + 4\ H+ + 4\ e- \qquad (1)$$

At potential values ranging from 1.1 V to 1.8 V the current density did not vary significantly with the potential. The observed passivity of the coated material is the result of the TiO_2-like film formed by the oxidation of TiN while at sites of imperfection in the coating the anodic behaviour of the substrate predominates. Finally, for potential values higher than 1.8 V, the current density augmented markedly as the potential was increased, attaining values higher than those measured for the uncoated material (greater than $10^{-5}A.cm^{-2}$). According to Rudenja et al. [31] this current increase could result from a region of enhanced oxidation of the TiN. These authors suggested that this accelerated oxide growth is probably associated with the observation that the charge carriers density of the TiO_2-like film formed by the oxidation of TiN is significantly higher than what has been observed for TiO_2 formed on pure Ti. It is noted that when these high potentials are reached, the coating has lost its characteristic golden colour.

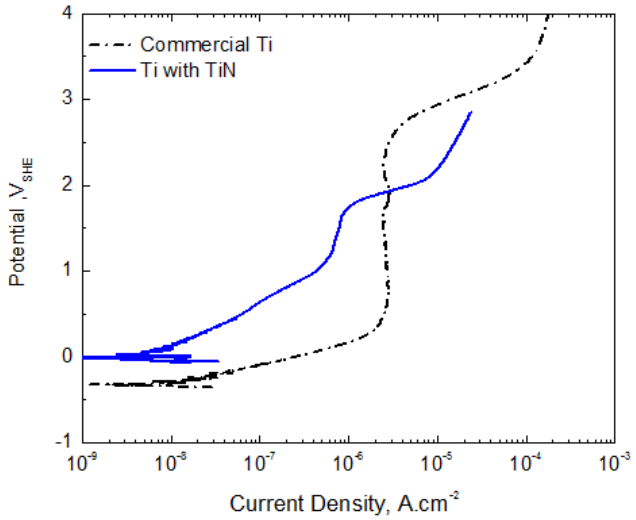

Figure 8. *Polarization curve of Ti and Ti coated with TiN in 0.1 M NaCl solution.*

Figure 9 shows the anodic polarization curves obtained for single-layer, double-layer and four-layer TiN coated titanium in 0.1M NaCl solution. As expected, a reduction of current

density was achieved as the number of applied layers was increased, due to the increase in coating thickness and the statistical reduction of the possibility of through-coating defects.

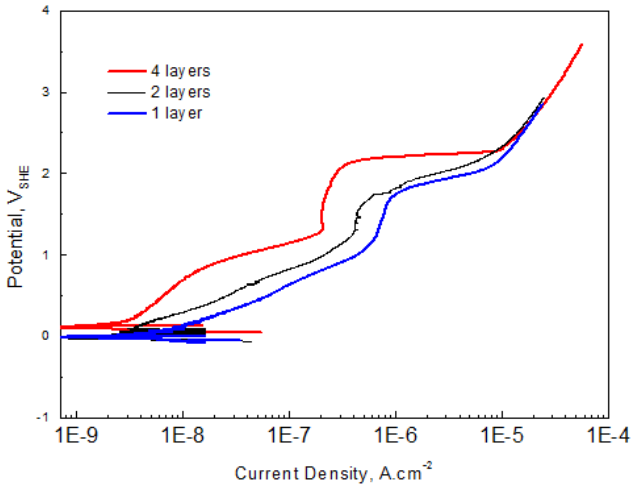

Figure 9. *Polarization curves for single-layer, double-layer and four-layer TiN coated Ti in 0.1M NaCl solution.*

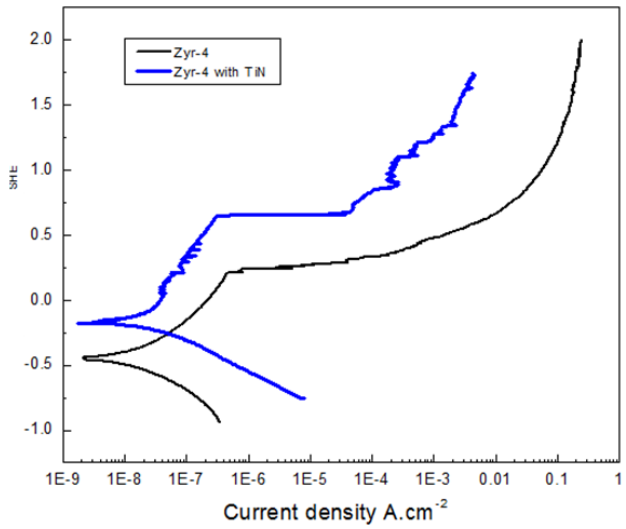

Figure 10. *Polarization curves for coated and uncoated Zyr-4 in 0.1 M NaCl solution.*

Zyr-4 and Zyr-4 coated with TiN

Figure 10 shows examples of the anodic polarization curves obtained for coated and non-coated Zyr-4 in a 0.1M NaCl solution. Both materials exhibited similar behaviour. When the potential was increased above the corrosion potential, a passive zone was observed, in which the current density was of the order of 10^{-7} A.cm^{-2} and did not change significantly with the potential. By further increasing the potential, a critical potential value was found, called the breaking potential or pitting potential, above which the current density showed a marked increase, indicating that passivity breakdown has already occurred and localized corrosion has been initiated on the metallic surface. One of the differences found between the coated and non-coated alloy was that the coated Zyr-4 exhibited a passive cd more than one order of magnitude lower than the uncoated material. Another difference was that the pitting potential value measured for the coated alloy was slightly higher than the one found for the uncoated alloy. The above observations indicate that the coating does not completely cover the metal surface and is unable to prevent localized corrosion of the Zyr-4 substrate, which occurred via through coating porosity. In consequence the anodic behaviour of the coated alloy is dominated by the influence of the substrate, the main difference being that the metallic surface area exposed to the solution is lower than half the area exposed in the non-coated samples.

3.5. Determination of the Electronic Conductivity of the TiN Coating

Determination of the electronic properties of surfaces films by means of anodic and cathodic polarization sweeps in solutions containing redox couples, such as FeII/FeIII, or $Fe(CN)_6^{-4}/Fe(CN)_6^{-3}$, has been widely used [33-34], because their reversible potential fall in about the middle of the passive region of many metals and alloys. Figure 11 shows the polarization curves obtained for coated and uncoated Ti in the redox system $K_4[Fe(CN)_6]/K_3[Fe(CN)_6]$. As is usually observed in films with semiconductive properties, the redox reaction showed a low exchange current density, lower than 10^{-6}A.cm^{-2}, and a marked symmetry of the anodic and cathodic branches on the Ti film.

On the other hand, the exchange current density measured on the TiN coating was found to be much higher than the one determined on the Ti film. It was also observed that when either anodic or cathodic overpotentials higher than of approximately 100mV were reached, both branches exhibited a limiting current density of the order 10-3 A.cm^{-2}. Figure 12 shows that the same behaviour was observed for coated and uncoated Zyr-4. The above results concerning the anodic and cathodic potential curves obtained for both Ti and Zyr-4 coated with TiN in the redox system $K_4[Fe(CN)_6]/K_3[Fe(CN)_6]$ indicate that the charge transfer reaction takes place very readily on the TiN surface and that the overall redox reaction is controlled by diffusion. Thus, it can be concluded that the TiN film has a high electronic conductivity.

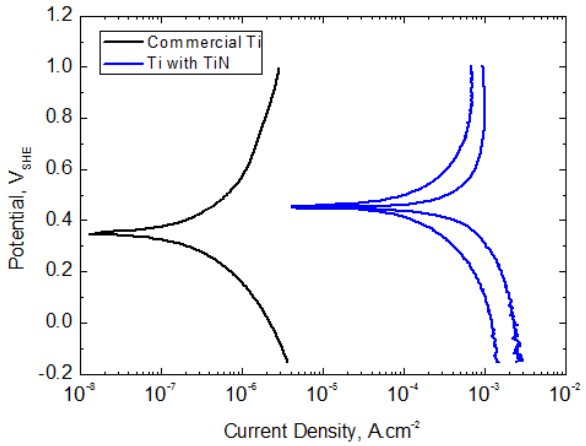

Figure 11. *Polarization curves measured for coated and uncoated Ti in [$K_4[Fe(CN)_6]$/M $K_3[Fe(CN)_6]$).*

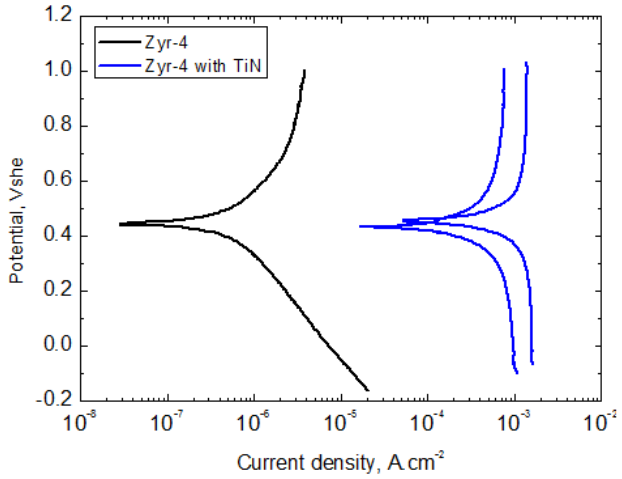

Figure 12. *Polarization curves measured for coated and uncoated Zry-4 in $[K_4[Fe(CN)_6]/M\ K_3[Fe(CN)_6])$.*

3.6. Galvanostatic Measurements

In order to check if the coated material is able to be used as an electrode through which a constant anodic current density has to be drain, a series of intensiostatic experiments were performed. In these experiments, a constant current density of 0.8 $A.cm^{-2}$ was applied and the evolution of the potential over time was recorded. Figure 13 shows the results obtained for single layer coated and non-coated commercial titanium. The duration of the test was 13,500 seconds (3h 45m). As soon as the current was applied, both the coated and non coated material showed a sudden potential increase but a stationary potential value was reached after an exposition of about 1000 seconds. Whereas the coated samples attained a stationary potential value of 3.5 V, the non-coated Ti samples, exhibited a stationary potential value higher than 10 V as a result of the insulating properties of the surface oxide film of TiO_2.

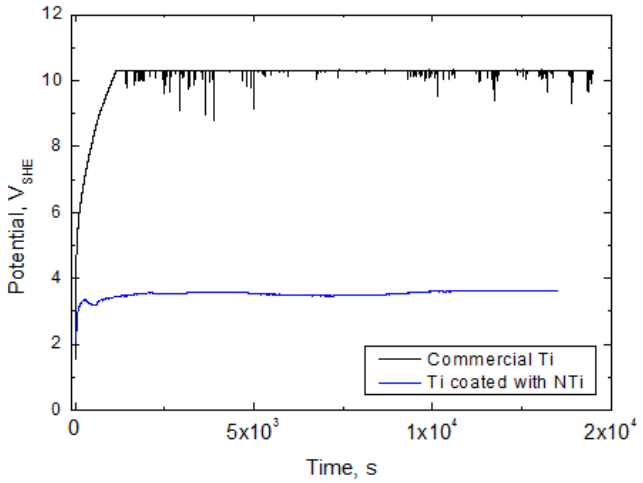

Figure 13. *Intensiostatic experiments for commercial Ti and single layer TiN coated Ti.*

In order to verify the stability of the coating over time, in another set of experiments both single layer and four-layer TiN coated titanium were exposed to the same experimental conditions during a 24 h period. Figure 14 shows an example of the obtained results. In the case of the single-layer coated specimens a stationary potential value of about 3.5V was measured up to four hours exposition, but for longer periods, the potential began to oscillate and showed an increasing trend, reaching after 24 h a value higher than 6.0V. It was also noted that the coating had lost its characteristic golden appearance. Moreover, it was also observed that the nitride film has been partially detached. In consequence, the potential showed a trend towards the values measured for the untreated samples. On the other hand, the four-layer specimens attained an initial potential of about 3.5 V but then the potential showed an increasing trend and oscillated between 3.5 V and 4.8 V during the whole exposition. However, it was also observed that the coating had lost its characteristic golden appearance and seems to be partially detached.

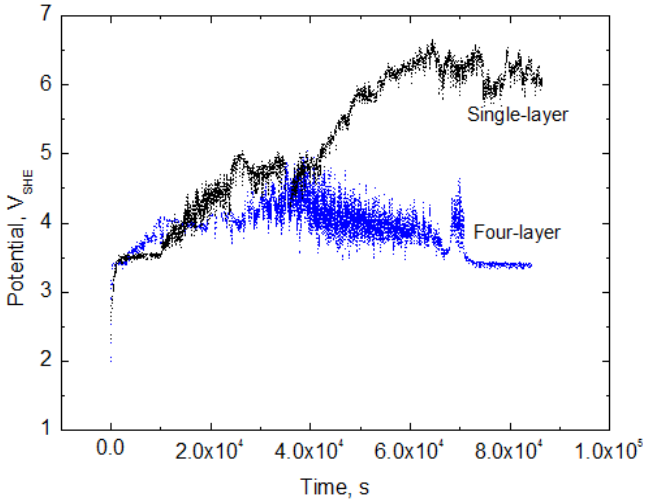

Figure 14. *Intensiostatic experiments for single layer and four- layer TiN coated Ti.*

4. Conclusions

The TiN monolayer coating has a mild effect on the good corrosion resistance of titanium and localized corrosion of Zyr-4 in aqueous chloride solutions. It is expected, a reduction of current density will be achieved with the increase of the number of applied layers, due to the increase in coating thickness and the statistical reduction of the possibility of through-coating defects.

Tests conducted in the presence of redox system Fe $(CN)_6^{-4}$/Fe $(CN)_6^{-3}$ show that the TiN coating gives Zyr-4 and commercial Ti features an electronic conductor. Therefore there is the possibility of using TiN in applications where the existence of a coating with good electrical conductivity applied on a substrate with insulating characteristics is required.

When a constant current density of 0.8 $A.cm^{-2}$ was applied the TiN coated titanium attained a potential value significantly lower than the non-coated titanium. However, the prolonged exposition to this high current density produce physical changes in the coating.

References

[1] V.M.C.A. Oliveira , C. Aguiar, A.M. Vazquez, A. Robin, M.J.R. Barboza, Improving corrosion resistance of Ti–6Al–4V alloy through plasma-assisted PVD deposited nitride coatings, Corros. Sci. 88, 2014 pp 317–327.

[2] Hui-Ping Feng, Cheng-Hsun Hsu, Jung-Kai Lu, Yih-Hsun Shy, Effects of PVD sputtered coatings on the corrosion resistance of AISI 304 stainless steel, Mat. Sci. and Engineering A347 2003 pp 123-129.

[3] D. Zhou, H. Peng, L. Zhu, H. Guo, Sh. Gong, Microstructure, hardness and corrosion behaviour of Ti/TiN multilayer coatings produced by plasma activated EB-PVD, Surf. and Coat. Tech., 258, November 2014, pp 102–107.

[4] S.A. Naghibi, K. Raeissi, M.H. Fathi, Corrosion and tribocorrosion behavior of Ti/TiN PVD coating on 316L stainless steel substrate in Ringer's solution, Mat. Chem. and Phys., 148, Issue 3, December 2014, pp 614–623.

[5] Holger Hoche, Stefan Groß, Matthias Oechsner, Development of new PVD coatings for magnesium alloys with improved corrosion properties, Surf. and Coat. Techn. 259, Part A, 25 November 2014, pp 102–108.

[6] C.V. Franco, L.C. Fontana, D. Bechi, A.E. Martinelli, J.L.R. Muzart, An electrochemical study of magnetron-sputtered Ti- and TiN-coated steel, Corros. Sci. 40, Issue 1, January 1998, pp 103–112.

[7] Wen-Jun Chou, Ge-Ping Yu, Jie-Hong Huang, Corrosion behavior of TiN-coated 304 stainless steel, Corros. Sci. 43 november 2001 pp 2023-2035.

[8] R.M. Souto, H. Alanyali, Electrochemical characteristics of steel coated with TiN and TiAlN coatings, Corros. Sci. 42 december 2000 pp 2201-2211.

[9] D.V. Tzaneva, V.I. Dimitrova, P.E. Hovsepyan, Influence of the formation conditions of TiN coatings on their electrochemical behaviour in sulphuric acid and sodium chloride solutions, Thin Solid Films, 297 february 1997 pp 178-184.

[10] A. Fossati, F. Borgioli, E. Galvanetto, T. Bacci, Corrosion resistance properties of plasma nitrided Ti–6Al–4V alloy in nitric acid solutions, Corros. Sci. 46 april 2004 pp 917-927.

[11] E. Galvanetto, F.P. Galliano, A. Fossati, F. Borgioli, Corrosion resistance properties of plasma nitrided Ti–6Al–4V alloy in hydrochloric acid solutions Corros. Sci. 44 july 2002 pp 1593-1606.

[12] S. Rossi, L. Fedrizzi, T. Bacci, G. Pradelli, Corrosion behaviour of glow discharge nitrided titanium alloys , Corros. Sci. 45 march 2003 pp 511-529.

[13] P.M. Perillo, Corrosion Behavior of Coatings of Titanium Nitride and Titanium-Titanium Nitride on Steel Substrates, Corrosion 62:2, 2006 pp 182-185.

[14] H. Alanyali and R.M. Souto, Research on the Corrosion Behavior of TiN-TiAlN Multilayer Coatings Deposited by Cathodic-Arc Ion Plating, Corrosion 59:10, 2003 pp851-853.

[15] Y.M. Chen, G.P. Yu, and J.H. Huang, Pinhole Enlargement during Electrochemical Porosity Measurement, Corrosion 58:10, 2002, pp 846-848.

[16] D Starosvetsky, I Gotman Corrosion behavior of titanium nitride coated Ni–Ti shape memory surgical alloy, Biomaterials, Volume 22, Issue 13, July 2001, pp 1853-1859.

[17] Ray W.Y. Poon, Joan P.Y. Ho, Xuanyong Liu, C.Y. Chung, Paul K. Chu, Kelvin W.K. Yeung, William W. Lu, Kenneth M.C. Cheung, Formation of titanium nitride barrier layer in nickel–titanium shape memory alloys by nitrogen plasma immersion ion implantation for better corrosion resistance Thin Solid Films, 488, Issues 1–2, 22 September 2005, pp 20-25

[18] B.Subramanian, R. Ananthakumar, M Jayachandran Microstructural, mechanical and electrochemical corrosion properties of sputtered titanium–aluminum–nitride films for bio-implants, Vacuum, 85, Issue 5, November 2010, pp 601-609.

[19] M. Tacikowski, J. Morgiel, M. Banaszek, K. Cymerman, T. Wierzchon, Structure and properties of diffusive titanium nitride layers produced by hybrid method on AZ91D magnesium Transactions of Nonferrous Metals Society of China, 24, Issue 9, September 2014, pp 2767-2775.

[20] F. Qi, Y.X. Leng, N. Huang, B. Bai, P.Ch. Zhang Surface modification of 17-4PH stainless steel by DC plasma nitriding and titanium nitride film duplex treatment, Nuclear Instruments and Methods in Physics Research Section B: Beam Interactions with Materials and Atoms, 257, Issues 1–2, April 2007, pp 416-419.

[21] Viorel-Aurel Şerban, Radu Alexandru Roşu, Alexandra Ioana Bucur, Doru Romulus Pascu, Deposition of titanium nitride layers by electric arc – Reactive plasma spraying method Applied Surface Science, 265, 15 January 2013, pp 245-249.

[22] S. Sedira, S. Achour, A. Avci, V. Eskizeybek, Physical deposition of carbon doped titanium nitride film by DC magnetron sputtering for metallic implant coating use Applied Surface Science, 295, 15 March 2014, pp 81-85.

[23] P .LeClair, G.P Berera, J.S Moodera, Titanium nitride thin films obtained by a modified physical vapor deposition process Thin Solid Films, 376, Issues 1–2, 1 November 2000, pp 9-15.

[24] I. Milosev, H. Strehblow, B. Navinsek, Comparison of TiN, ZrN and CrN hard nitride coatings: Electrochemical and thermal oxidation, Thin Solid Films 303, july 1997 pp 246-254.

[25] L.T. Cunha, P. Pedrosa, C.J. Tavares, E. Alves, F. Vaz, C. Fonseca, The role of composition, morphology and crystalline structure in the electrochemical behaviour of TiNx thin films for dry electrode sensor materials, Electrochim. Acta 55(1), december 2009, pp 59-67

[26] C. Liu, A. Leyland, Q. Bi, A. Matthews, Corrosion resistance of multi-layered plasma-assisted physical vapour deposition TiN and CrN coatings, Surf. and Coat. Techn. 141 june 2001 pp 164-173.

[27] H. Pulker, “Wear and Corrosion Resistance Coatings by CVD and PVD” E. Horwood, Halsted Press (Chichester, New York) 1989.

[28] M.V. Kuznetsov, Ju.F. Zhuravlev, V.A. Gubanov, XPS study of the nitrides, oxides and oxynitrides of titanium, J. Electron. Spectroscopy 58 ,1992, pp 1-9.

[29] D. M. Devia, J. Restrepo, A. Ruden, J.M. González, F. Sequeda, and P.J.Arango, The Tribological Characteristics of TiN, TiC, TiC/TiN Films Prepared by Reactive Pulsed Arc Evaporation Technique, Society of Vacuum Coaters 505 2009, pp. 856-7188.

[30] P.Prieto and R. E. Kirby, X-ray photoelectron spectroscopy study of the difference between reactively evaporated and direct sputter-deposited TiN films and their oxidation properties J. Vac. Sci. Technol. A 13, 1995 pp 2819-2822.

[31] S.Rudenja, J. Pan, I. Odnevall Wallinder, C. Leygraf, and P. Kulu, Passivation and Anodic Oxidation of Duplex TiN Coating on Stainless Steel, J. Electrochem. Soc., 146 (11) 1999, pp 4082-4086.

[32] [32 K. Azumi, S. Watanabe, M. Seo, I. Saeki, Y. Inocuchi, P. James and W. Smyrl, Characterization of anodic oxide film formed on tin coating in neutral borate buffer solution Corros. Sci., 40, N°8 august 1998, pp 1363-1377.

[33] P.E. Manning, D.J. Duquette, The effect of temperature (25°–289°C) on pit initiation in single phase and duplex 304L stainless steels in 100 ppm Cl− solution, Corros. Sci. 20, 1980 pp 597-609.

[34] R.M. Carranza, M.G. Alvarez, The effect of temperature on the passive film properties and pitting behaviour of a Fe-Cr-Ni alloy, Corros. Sci. 38 june 1996, pp 909-925.